Targeted drug delivery to tumor vasculature by a carbohydrate mimetic peptide

Shingo Hatakeyama[a], Kazuhiro Sugihara[b,1], Toshiaki K. Shibata[a], Jun Nakayama[c], Tomoya O. Akama[a], Naoaki Tamura[a], Shuk-Man Wong[a], Andrey A. Bobkov[a], Yutaka Takano[a], Chikara Ohyama[d], Minoru Fukuda[a], and Michiko N. Fukuda[a,1]

[a]Tumor Microenvironment Program, Cancer Center, Sanford-Burnham Medical Research Institute, La Jolla, CA 92037; [b]Department of Gynecology and Obstetrics, Hamamatsu University School of Medicine, Hamamatsu 431-3192, Japan; [c]Department of Molecular Pathology, Shinshu University Graduate School of Medicine, Matsumoto 390-8621, Japan; and [d]Department of Urology, Hirosaki University School of Medicine, Hirosaki 036-8243, Japan

Edited* by Carolyn R. Bertozzi, University of California, Berkeley, CA, and approved October 3, 2011 (received for review March 29, 2011)

Although numerous carbohydrates play significant roles in mammalian cells, carbohydrate-based drug discovery has not been explored due to the technical difficulty of chemically synthesizing complex carbohydrate structures. Previously, we identified a series of carbohydrate mimetic peptides and found that a 7-mer peptide, designated I-peptide, inhibits hematogenous carbohydrate-dependent cancer cell colonization. During analysis of the endothelial surface receptor for I-peptide, we found that I-peptide bound to annexin 1 (Anxa1). Because Anxa1 is a highly specific tumor vasculature surface marker, we hypothesized that an I-peptide-like peptide could target anticancer drugs to the tumor vasculature. This study identifies IFLLWQR peptide, designated IF7, as homing to tumors. When synthetic IF7 peptide was conjugated to fluorescent Alexa 488 (A488) and injected intravenously into tumor-bearing mice, IF7-A488 targeted tumors within minutes. IF7 conjugated to the potent anticancer drug SN-38 and injected intravenously into nude mice carrying human colon HCT116 tumors efficiently suppressed tumor growth at low dosages with no apparent side effects. These results suggest that IF7 serves as an efficient drug delivery vehicle by targeting Anxa1 expressed on the surface of tumor vasculature. Given its extremely specific tumor-targeting activity, IF7 may represent a clinically relevant vehicle for anticancer drugs.

angiogenesis | carbohydrate binding protein | geldanamycin | phage display | chemiluminescence

Technical advances in genomics and proteomics together with automated chemical synthesis of DNA and proteins have greatly contributed to progress in biomedicine. By contrast, understanding the role of carbohydrates has lagged due to lack of advanced technologies. Currently, for example, we cannot produce recombinant or amplifiable carbohydrates or chemically synthesize complex carbohydrates automatically. Consequently, carbohydrate-based drug discovery has been largely unexplored despite the fact that cancer malignancy is closely associated with carbohydrate structures found on the tumor cell surface (1, 2). To move beyond this dilemma, we and others have employed peptide-displaying phage technology and identified peptides that function as carbohydrate ligands (3–9). For example, we screened a phage library of linear 7-mer peptides using monoclonal anti-Lewis A antibody (clone 7LE) and obtained a series of peptides with the consensus sequence IXLLXXR (3). Among them, IELLQAR, or I-peptide, was the most potent binder to selectins, suggesting that selectins recognize a Lewis A mimetic peptide as their ligand. Synthetic I-peptide injected intravenously into mice inhibited lung colonization of B16FT-IIIM cells, a line derived from B16 melanoma cells transfected with fucosyltransferase, FUT-3, enabling expression of sialyl Lewis X antigen, whereas parental B16 cells do not express sialyl Lewis X antigen and poorly colonize the lung (3, 10, 11). However, sialyl Lewis X-dependent B16FT-IIIM colonization occurred in E-selectin/P-selectin doubly-deficient mutant mice, and I-peptide inhibited that colonization, suggesting the presence of a yet unknown I-peptide receptor distinct from E- or P-selectins (11). We then isolated the putative receptor by I-peptide affinity chromatography and subjected it to proteomic analysis, which identified the I-peptide receptor as a pre-mRNA splicing factor (12). During these experiments, we found unexpectedly that I-peptide binds to a 15 kDa fragment of annexin 1 (Anxa1) (12).

A rigorous subtractive proteomics analysis indicates that Anxa1, among the many tumor vasculature markers previously described (13, 14), is a highly specific marker of the tumor vasculature surface (15). Anxa1 belongs to the large annexin family and is expressed in numerous cell types. Annexins bind to phospholipids in a calcium-dependent manner, providing a link between calcium-dependent signaling and membrane function (16, 17). Although annexins lack signal sequences for secretion, some family members have been found on cell surface. By forming networks on the membrane surface, annexins participate in events ranging from membrane dynamics to cell differentiation and migration (16). In resting neutrophils, Anxa1 is cytoplasmic, whereas upon adhesion to endothelial cells Anxa1 is externalized and binds through its N terminus to formyl peptide receptor 2 (FPR2) (18, 19). Phenotypes exhibited by Anxa1 null mice suggest that Anxa1 mediates some antiinflammatory activities of glucocorticoids (20).

Anxa1 was detected on the surface of endothelial cells that are part of the tumor vasculature in several tumor types in mice and humans (15). Because I-peptide bound to Anxa1 fragments (12), we hypothesized that I-peptide-related peptide could serve as a tumor-specific drug delivery vehicle. In this study, we rescreened a series of phage clones displaying I-peptide-related sequences for tumor-targeting activity. Here we describe a specific Anxa1-binding peptide, designated IF7, as a highly efficient targeting vehicle for delivering anticancer drugs to a tumor in vivo in the mouse.

Results

Identification of the Tumor-Targeting and Anxa1-Binding Peptide. Because I-peptide targets normal lung through pre-mRNA splicing factor and it is likely targets the tumor vasculature through Anxa1 (12) (Fig. S1*A*), we looked for a peptide sequence specifically targeting tumor but not normal lung vasculature. Organ targeting of phage clones intravenously injected into tumor-bearing mice suggested that IFLLWQR, designated IF7, specifically targets tumor but not normal lung tissue (Fig. 1*A*). IF7 phage bound to

Author contributions: S.H., K.S., T.O.A., M.F., and M.N.F. designed research; S.H., T.K.S., J.N., N.T., S.-M.W., A.A.B., and M.N.F. performed research; S.H., N.T., A.A.B., Y.T., C.O., and M.N.F. contributed new reagents/analytic tools; S.H., K.S., T.K.S., J.N., T.O.A., M.F., and M.N.F. analyzed data; and K.S., T.K.S., J.N., and M.N.F. wrote the paper.

The authors declare no conflict of interest.

*This Direct Submission article had a prearranged editor.

Freely available online through the PNAS open access option.

[1]To whom correspondence may be addressed. E-mail: michiko@sanfordburnham.org or sugihara@hama-med.ac.jp.

This article contains supporting information online at www.pnas.org/lookup/suppl/doi:10.1073/pnas.1105057108/-/DCSupplemental.

recombinant Anxa1-His$_6$ protein, whereas it did not bind to His$_6$-Anxa1 (Fig. S1*B*). IF7 phage binding to Anxa1-His$_6$ was inhibited by a rabbit anti-Anxa1 antibody raised against the N terminus (Fig. S1*C*). IF7 phage did not bind to Anxa1 mutant protein lacking the N-terminal 12 amino acids (Fig. S1*D*), strongly suggesting that IF7 binds to that region. When the anti-Anxa1 antibody, which inhibited binding of IF7 phage to Anxa1-His$_6$ in a plate assay (Fig. S1*C*), was injected prior to IF7 phage injection, tumor targeting by IF7 phage in the mouse was completely inhibited by this antibody (Fig. 1*B*), strongly suggesting that IF7 binds to the tumor vasculature through Anxa1 expressed on the endothelial cell surface (15). Although we previously detected low levels of Anxa1 fragment in lung by biotinylation (12), we could not detect IF7 targeting to the lung in tumor-bearing mice using an in vivo phage targeting assay (Fig. 1*B*), suggesting that Anxa1 levels on the surface of lung endothelial cells are significantly lower than those expressed on the tumor vasculature.

IF7 peptide was chemically synthesized and was conjugated with fluorescent Alexa 488 (Fig. S2). The conjugate, designated IF7-A488, bound to Anxa1-His$_6$ protein in a plate assay, whereas RQ7-A488 (Alexa 488 conjugated to reverse IF7 or RQWLLFI) did not (Fig. 2*A*). IF7 binding to Anxa1 was confirmed by isothermal titration assays, in which stoichiometry suggested that IF7 binds to Anxa1 dimer (Fig. S3). Multivalent synthetic carbohydrates bound to recombinant Anxa1-His$_6$ protein (Fig. 2*B*), and that binding was inhibited by monomeric IF7 peptide but not by RQ7 (Fig. 2*C*).

In Vivo Tumor-Targeting Activity by IF7. To test in vivo tumor vasculature-targeting activity by IF7, tumors were produced in a dorsal skinfold chamber installed on nude mice (21). When IF7-A488 was injected through the tail vein and tumor fluorescence monitored microscopically, fluorescence signals appeared in the tumor within 1 min of injection, reached a plateau in 9 min, and

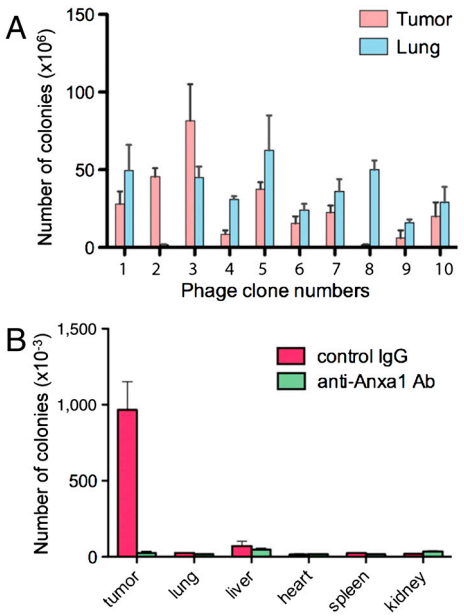

Fig. 1. Identification of a peptide sequence with tumor vasculature-targeting activity in vivo. (*A*) In vivo phage targeting in B16 tumor-bearing mice. Phage clones each displaying I-peptide and IF7 have been described (3). The number of bacterial colonies transformed by phage recovered from the tumor or lung was determined. Peptide sequences displayed by clones 1–10 are: IELLQAR [1], IFLLWQR [2], IILLQAR [3], IDLMQAR [4], ISLLQAR [5], FSLLDAR [6], ISLLGAR [7], PLWRPSR [8], LLLMQLR [9], and LYLQRLR [10]. (*B*) In vivo tumor and organ targeting activity of IFLLWQR-displaying phage. Phage was injected into B16 tumor-bearing mice preinjected with anti-Anxa1 (N-19) antibody or with control rabbit IgG.

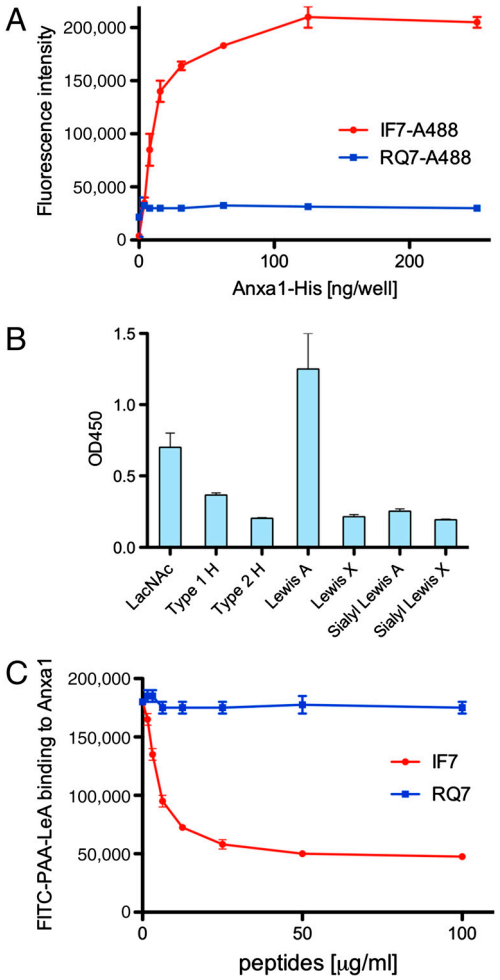

Fig. 2. In vitro plate assay for binding of IF7 peptides and polymeric carbohydrates. (*A*) Binding of IF7-A488 and control RQ7-A488 to recombinant Anxa1-His$_6$ protein produced by bacteria. (*B*) Binding of various carbohydrate antigens conjugated to biotinylated polyacrylamide (PAA) with Anxa1-His$_6$ protein. Recombinant Anxa1-His$_6$ protein was coated on a plastic wellls, and the binding of biotinylated PAA-carbohydrate was added to the wells. LacNAc, Galβ1 → 4GlcNAcβ1 →; Type 1 H, Fucα1 → 2Galβ1 → 3GlcNAcβ1 →; Type 2 H, Fucα1 → 2Galβ1 → 4GlcNAcβ1 →; Lewis A, Galβ1 → β(Fucα1 → 4) GlcNAcβ1 →; Lewis X, Galβ1 → 4(Fucα1 → 3)GlcNAcβ1 →; Sialyl Lewis A, NeuNAcα2 → 3Galβ1 → 3(Fucα1 → 4)GlcNAcβ1 →; Sialyl Lewis X, NeuNAcα2 → 3Galβ1 → 4(Fucα1 → 3)GlcNAcβ1 →. (*C*) Effect of IF7 and control RQ7 on binding of FITC-labeled polyacrylamide-Lewis A oligosaccharide to Anxa1-His$_6$ protein.

remained high for 40 min or until the experiment was terminated (Fig. 3 *A* and *B*). By contrast, control peptide RQ7-A488 signals remained at background levels. When normal rabbit IgG was injected prior to IF7-A488 injection, tumor targeting of IF7-A488 was not altered. On the other hand, when the anti-Anxa1 antibody, which inhibited binding of IF7 phage to Anxa1-His$_6$ (Fig. S1*C*), was injected prior to IF7-A488 injection, fluorescence signals in tumors were significantly reduced. Tissue sections prepared from the tumor 20 min after injection showed vascular staining by IF7-A488, but not by RQ7-A488 (Fig. 3*C*). These results support the hypothesis that IF7 targets tumors through Anxa1 expressed on the endothelial cell surface.

Effect of Anticancer Drugs Conjugated with IF7. We next asked whether IF7 could deliver a drug to the tumor and suppress tumor growth in vivo. We conjugated IF7 with an apoptosis-inducing anticancer drug 17-AAG (GA), a geldanamycin analogue (22, 23) (Fig. S2). When the IF7-GA was injected intravenously

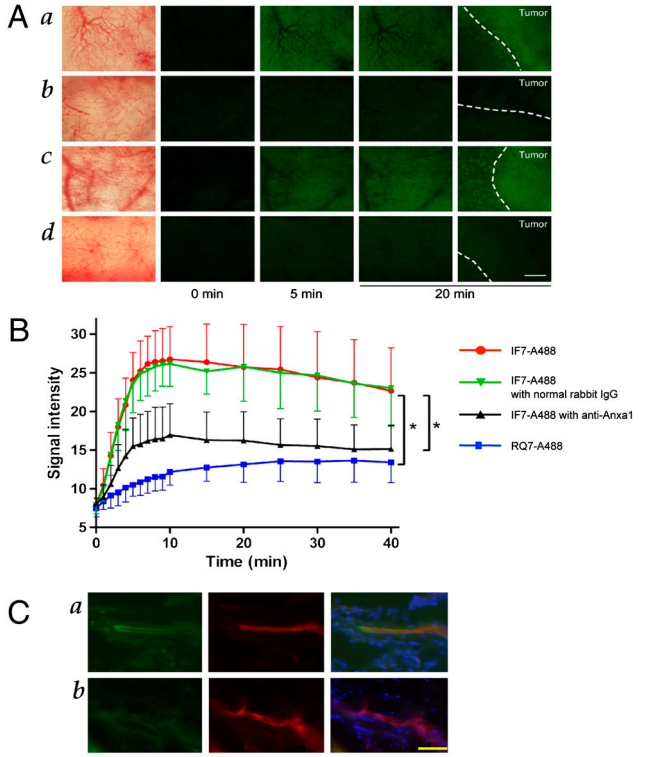

Fig. 3. In vivo targeting of IF7-A488 to tumors. (*A*) LLC tumors were allowed to become vascularized for 3 d in a dorsal skinfold chamber window in nude mice (21). Mice were injected with 100 μL of 50 μM IF7-A488 (*a*) or RQ7-A488 (*b*) in 5% glucose in water. Green fluorescence signals were recorded by video under a fluorescence microscope up to 40 min postinjection. IF7-A488 was also injected into tumor-bearing mice preinjected with rabbit IgG (*c*) or with rabbit anti-Anxa1 (N-19) antibody (*d*). From left: bright field before injection, and fluorescence at 0, 5, and 20 min after IF7-A488 injection. Far right boxes indicate the boundary between the tumor and stroma at 20 min (Scale bar, 500 μm). (*B*) Quantitative analysis of fluorescence during the course of the analysis shown in (*A*).-Intensity of fluorescence was determined using Image *J* program. Error bars represent SD ($n = 3$). Asterisks show statistical significance or $p < 0.0001$ in a *t*-test. (*C*) Fluorescence micrographs of tumor sections 20 min after injection with IF7-A488 (*a*) or RQ7-A488 (*b*), coinjected with Texas-red conjugated tomato lectin. Shown are IF7-A488 or RQ7-A488 (left), Texas-red tomato lectin (middle), and the merge with DAPI nuclear staining (right). (Scale bar,50 μm).

into melanoma, lung carcinoma, prostate cancer, and breast cancer model mice, tumor growth was suppressed: tumors from IF7-GA-treated mice were significantly smaller than those from control mice (Fig. S4*A*). It should be noted that the dose of 17-AAG used as IF7-GA was 0.13 μmoles/injection or 5 mg/kg, whereas 50–75 mg/kg 17-AAG was used in previous studies of mouse tumor models (24–26). Histological analysis showed that while tumors from control mice were actively growing around blood vessels, cells in tumors from IF7-GA-treated mice showed clear signs of apoptosis along vessels and morphologically apparent necrosis of blood vessels (Fig. S4*B*), indicative of a GA effect against tumor and tumor endothelial cells (22, 27). Blood tests from all mice used in these experiments showed no side effect in liver function, kidney function, and blood cell count (Fig. S5*A*). These results indicate that, as proof-of-principle, IF7-conjugated anticancer drug suppress tumor growth regardless of tumor types at the dosage lower than that of unconjugated drug.

In the above described experiments, however, IF7-GA did not suppress tumor growth completely. We hypothesized that such moderate activity is due to the limited potency of 17-AAG, a drug that induces tumor cell apoptosis by inhibiting Hsp-90 (28, 29). We therefore conjugated IF7 to a more potent anticancer drug, SN-38, which inhibits topoisomerase I (30, 31). To ensure the release of SN-38 upon delivery to the tumor, IF7 was conjugated to SN-38 through an esterase-cleavable linker (32) (Fig. S6). We also added two arginine residues after the cystein on IF7 to create IFLLWQR-C-RR, or IF7C(RR), to increase conjugate solubility, as IF7C-SN38 was poorly soluble in an aqueous solution. We found that IF7C(RR)-SN38 bound to recombinant Anxa1 (Fig. S7*A*) and used it in the remaining experiments. To monitor tumor growth accurately in vivo, we employed luciferase-based cancer imaging. The colon cancer cell line HCT116, which is susceptible to SN-38 cell killing (33), was infected with lentivirus driving luciferase expression, enabling visualization of cells by the Xenogen imager. We confirmed that IF7C(RR) targeted HCT116-luc tumors in vivo (Fig. S7*B*). Because our preliminary experiments suggested that daily injections are required to effectively suppress HCT116-Luc tumor growth by IF7C(RR)-SN38, we injected IF7C(RR)-SN38 intravenously daily into HCT116-luc tumor-bearing mice. When IF7C(RR)-SN38 was injected into nude mice bearing large HCT116-Luc tumors, tumor size was dramatically reduced, whereas tumor growth in control mice injected with RQ7C(RR)-SN38 was unchanged, as demonstrated by both photon number and caliper measurements (Fig. 4 *A* and *B*). It is noteworthy that IF7-SN38 injections administered here were 0.13 μmoles/injection or 6.5 μmoles/kg (13.9 mg)/kg, whereas SN-38 conjugated with a peptide lacking tumor vasculature-targeting activity was used at 95 mg/kg in a previous study (32).

To confirm antitumor activity of IF7C(RR)-SN38, we reduced the levels of IF7C(RR)-SN38 administered. We observed that

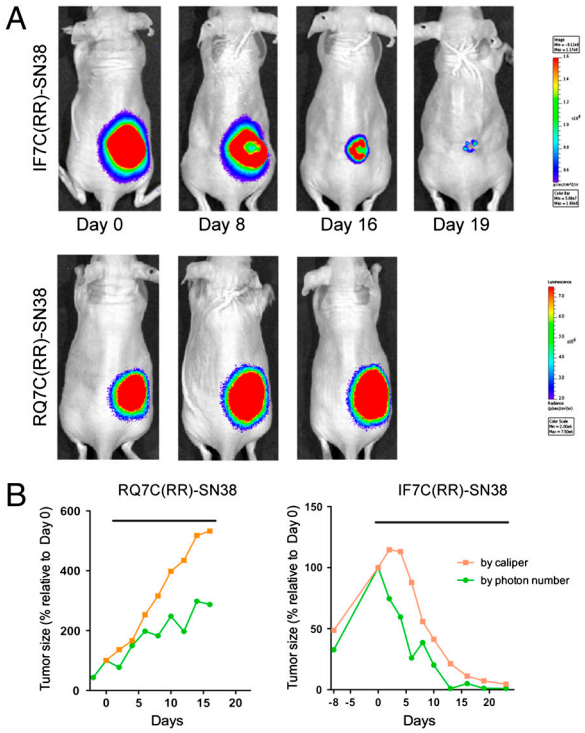

Fig. 4. Effect of IF7C(RR)-SN38 on HCT116-Luc tumors in nude mice. (*A*) Chemiluminescence images of a large HCT116-Luc tumor in a mouse each injected with IF7C(RR)-SN38 or RQ7C(RR)-SN38. When the tumor reached a photon size of 1.8e+10, daily injection of peptide-conjugated SN-38 was initiated. IF7C(RR)-SN38 (0.13 μmoles) was dissolved in 10 μL dimethylsulfoxide and diluted with 100 μL of 5% glucose, which was then injected intravenously into mice through the tail vein. Tumor size is expressed as relative to that observed on day 0, which is set at 100%. On day 19, the photon number was 2.0e+08 in IF7C(RR)-SN38 injected mouse. In control or RQ7C(RR)-SN38 injected mouse, experiment was stopped on day 16 as the tumor size exceeded 2 cm^3. (*B*) Tumor size measured by photon numbers and caliper measurement of the same animal shown in box (*A*). The period during which drug was injected daily is indicated by the black bar.

daily injection of IF7C(RR)-SN38 at 0.033 μmoles/injection or 1.63 μmoles/kg (3.48 mg/kg) effectively suppressed growth of HCT116-Luc tumors (Fig. 5), whereas administration RQ7C (RR)-SN38 or unconjugated SN-38 did not show this effect. Histological examination of tumors treated with IF7C(RR)-SN38 revealed significant necrosis and apoptosis (Fig. S8). Blood tests showed no sign of side effects in IF7C(RR)-SN38-injected mice (Fig. S5*B*).

Discussion

Although the idea of targeted drug delivery has been discussed for some time, a universal cancer targeting strategy is not yet in sight. Monoclonal antibody therapy is one means of targeting drugs (34); however, humanized monoclonal antibodies are required for clinical application, an effort that is laborious and therefore expensive. On the other hand, peptides are easily synthesized, and synthesized peptides can be readily modified. A short 7-mer peptide such as IF7 likely would not function as an antigen, and therefore concerns regarding immune reactions in patients injected with IF7 are minimal. IF7 peptide's tumor-targeting activity is unprecedented: in mice, we detected intravenously injected IF7 in the tumor within a few minutes of injection (Fig. 3 *A* and *B*), a speed that may exceed that achieved by antibodies.

Annexin family proteins localize to endothelial caveolae surfaces and are internalized through endocytosis (35). Antibodies bound to an endothelial caveoli protein are reportedly efficiently transported to the basal surface and released to the stroma below (36). Our results using IF7C(RR)-conjugated poly-L-lysine suggest similar apical to basal transport of IF7-conjugated poly-L-lysine through endothelial cells in vitro and in vivo (Fig. S7*B*, Fig. S9). In these processes in vivo, the peptide moiety of the conjugate would likely be digested by proteases, allowing the anticancer drug to freely penetrate tumor cells. This hypothesis is consistent with histological observations showing that cells located around the vasculature underwent apoptosis and necrosis in tumor-bearing mice injected with IF7-GA (Fig. S4*B*).

Susceptibility to proteases is considered by some a disadvantage of peptide-based therapeutics (37, 38). Indeed, pharmacokinetics of IF7C(RR)-SN38 and IF7C-SN38 suggested that these peptides are susceptible to proteases in mouse plasma (Fig. S10 *A* and *B*). Because the intended role of IF7 is as a drug delivery vehicle, IF7-conjugated drug should remain intact until it reaches the tumor vasculature, where it can then be degraded. We speculate that at least some, if not all, IF7-conjugated drug is delivered to the tumor before proteolysis occurs, because IF7-GA and IF7C(RR)-SN38 exhibited antitumor activities at considerably lower doses than those required without IF7 (Figs. 4 and 5, Fig. S4*A*) (24–26, 32). Antitumor activity by IF7C(RR)-SN38 relative to that by control RQ7C(RR)-SN38 may not be attributable to the stability of this peptide over control peptide, because both disappeared from mouse plasma at comparable speed (Fig. S10*A*).

The efficacy of a peptide-conjugated anticancer drug also depends on the chemistry of conjugation. Here, we used an esterase-resistant linker for GA and an esterase-cleavable linker for SN-38. When IF7C(RR)-SN38 was incubated at 37 °C with mouse plasma, as much as 50% of SN-38 was released from the conjugate within 10 min (Fig. S10*C*). As it takes 9 min for IF7 to target the tumor (Fig. 3*B*), this suggests that tumor growth suppression (Figs. 4 and 5) was achieved by IF7C(RR)-SN38 survived in the initial 10 min window upon intravenous injection. Although IF7C(RR)-SN38 may be more stable in human plasma, which exhibits weaker esterase activity than does mouse plasma, future studies should address ways to both enhance drug stability in the circulation and promote efficient drug release in tumor tissue.

Annexins exhibit N termini unique to each family member and an evolutionarily conserved core domain (39). In this study, we present data suggesting that IF7 binds to the Anxa1 N terminus (Fig. S1 *B–D*, Fig. 3 *A* and *B*). The Anxa1 N-terminal amino acid sequence is completely conserved between mouse and humans. Thus it is likely that IF7 would bind to human Anxa1 expressed on tumor vasculature.

In this study, we have explored therapeutic potential of Anxa1-binding peptide as a cancer treatment. The extremely efficient tumor vasculature-targeting activity by IF7 and possibility for further improvement of this technology warrant evaluation of clinical efficacy of anticancer drugs conjugated to Anxa1-binding peptides in patients.

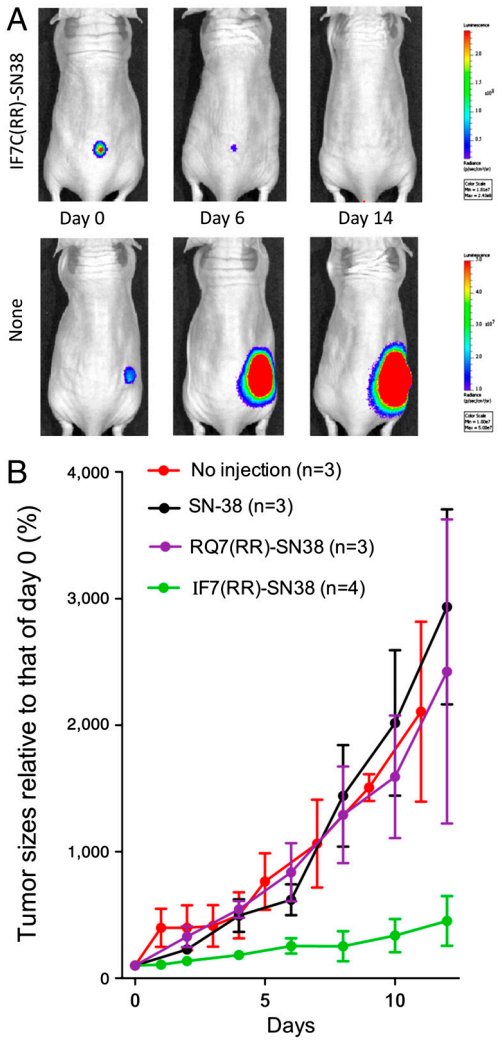

Fig. 5. Effect of low doses of IF7C(RR)-SN38 on HCT116-Luc tumors. (*A*) Images of HCT116-Luc tumors visualized by luciferase activity. (*B*) Tumor size measured by photon numbers in animals injected daily with low doses IF7C (RR)-SN38 or RQ7C(RR)-SN38. Mice with HCT116-Luc tumors (photon numbers, 1.0e+08) were subjected to daily injection of IF7C(RR)-SN38, RQC (RR)-SN38, or SN-38, all of which were injected at 0.033 μmoles/injection or 3.5 mg/kg.

Materials and Methods

Peptides, Phage Clones, and Antibodies. Peptides were synthesized by GenScript. Rabbit anti-Anxa1 antibody raised against residues 235–299 of human Anxa1 (H-65), rabbit anti-Anxa1 antibody raised against N terminus of human Anxa1 (N-19) were from Santa Cruz Biotechnologies. Rabbit anti-Anxa1 antibody raised against full-length recombinant human Anxa1 protein was from Zymed. Phage clones each displaying I-peptide and IF7 were described previously (3).

Use of Vertebrate Animals. Mouse protocols were approved by Institutional Review Committees at Sanford-Burnham Medical Research Institute.

In Vivo Phage Targeting. Mouse melanoma B16F1 cells (2×10^5 cells/100 μL PBS) were injected subcutaneously into the dorsal flank of C57BL/6 female mice (8–10 w old). Ten days later, I-peptide displaying phage clones or each clone displaying I-peptide related sequence (1×10^5 pfu) in 100 μL PBS was injected intravenously. In a separate set of experiments, rabbit anti-Anxa1 antibody (N-19) or rabbit IgG (20 μg IgG) was injected 15 min prior to phage injection. The mouse was perfused with Tris buffer saline (TBS) containing 1 mM $CaCl_2$, and tumor and lung tissue was isolated. Tissue homogenates (100 mg protein) were incubated with competent K91 bacteria, and plated on LB agar containing tetracycline (10 μg/mL) and kanamycin (100 μg/mL). Colonies appearing on an agar plate after culturing at 37 °C for 20 h were counted.

Preparation of Recombinant Anxa1-His$_6$, His$_6$-Anxa1, and Δ12Anxa1-His$_6$ Proteins. Full-length cDNA encoding Anxa1 from Invitrogen was subcloned at the NdeI and XhoI sites into pET29a vector (Novagen) to produce Anxa1-His$_6$. The *Escherichia coli* BL21 (DE3) strain was transformed with vector DNA, and transformants were cultured in LB medium containing kanamycin (30 μg/mL) to OD600 0.6 ~ 1.0. Anxa1-His$_6$ protein was induced by treatment with 1 mM isopropyl-thio-galactoside for 3 h at 37 °C. Anxa1-Hi$_6$ protein was extracted from bacteria with 20 mM TrisHCl buffer, pH 7.9, containing 500 mM NaCl and 5 mM imidazole, and applied to a Nickel Nitriloacetic acid (NTA) column. After washing with the same buffer containing 250 mM NaCl and 30 mM imidazole, Anxa1-His$_6$ protein was eluted from the column with the same buffer containing 300 mM imidazole. Protein purity was verified by SDS-PAGE followed by Coomassie blue staining. His$_6$-Anxa1 protein was similarly prepared except that Anxa1 cDNA was subcloned into the pET28a vector (Novagen). The N-terminal deletion mutant Δ12Anxa1-His$_6$ was prepared by PCR deletion of Anxa1 cDNA in the pET29a vector using Δ12 [AGATATACATATGCTTGAAAATCAAGAACAGGAATA (NdeI site underlined) and T7T primers]. The product was digested by NdeI and XhoI, subcloned into pET29a, and verified by DNA sequencing.

Phage Binding Assay on Recombinant Anxa1 Proteins With or Without Anti-Anxa1 Antibodies. Anxa1-His$_6$ and His$_6$-Anxa1 proteins were prepared as described. Each protein was added to wells of an ELISA 96-well-plate at 20 μg/mL and left at 4 °C for 20 h. After washing with TBSTC (20 mM Tris-HCl buffer, pH 7.4, containing 100 mM NaCl, 0.1% Tween 20 and 1 mM $CaCl_2$), wells were blocked with TBSTC containing 1% bovine serum albumin. Anti-Anxa1 antibody or control irrelevant rabbit antibody (4 μg each) was added to each well and incubated for 15 min. IF7 peptide-displaying phage (1×10^6 CFU) was then added and incubated at room temperature for 15 min. After washing wells with TBSTC, phage bound to each well was counted using the colony forming assay described above.

Binding of IF7-A488 to Anxa1-His$_6$ Protein. Wells of a black 384-well plate (Greiner bio-one) were coated with serially diluted recombinant IF7-His$_6$ protein. IF7-A488 or RQ7-A488 was dissolved at 4 μg/mL in 10 mM Tris-HCl buffer, pH 7.4, containing 1 mM $CaCl_2$ and 0.05% Tween 20, and was added to wells. After washing the plate, fluorescence was measured by a Molecular Devices Analyst HT plate reader. Analysis of inhibition of binding of Lewis A oligosaccharide to Anxa1-His$_6$ by IF7 and control RQ7 peptide was carried out using FITC-conjugated polyacrylamide-Lewis A (Glycotech) as described above. IF7C(RR)-SN38 and RQ7C(RR)-SN38 binding assays were similarly performed.

In Vivo Imaging of IF7-A488 in Dorsal Skinfold Chamber Window. A Lewis lung carcinoma (LLC) tumor was produced in a donor nude mouse by subcutaneous injection, and small piece of tumor (less than 1 mm^3) was transplanted to a dorsal skinfold chamber in a recipient nude mouse (8–10 w female Balb/c nude) as described (21, 36). Three days later, the mouse was anesthetized by peritoneal injection of 1.25% 2,2,2-Tribromoethanol (25 μL/g). IF7-A488 or RQ7-A488 (100 μL; 50 mM in 5% glucose solution) was injected through the tail vein. Intravital Alexa 488 signals in the tumor were detected and recorded by a Zeiss Axioplan fluorescence microscope and a digital camera system (DP70 and DP controller, Olympus). For inhibition assays, 20 ug each rabbit anti-Anxa1 antibody (N-19) or rabbit IgG was injected 15 min prior to IF7-A488 injection. Signal intensity in the tumor from 0 min to 40 min was measured by Image J (NIH). After 10 min, irradiation of specimens by a UV lamp was limited only to times when photos were taken to avoid fluorescence bleaching. The tumor was isolated from the dorsal skin folder chamber, fixed with 4% paraformaldehyde at room temperature for 15 min, immersed in Optimal Cutting Temperature (OCT) compound, and cryosections were made. Frozen sections were overlaid with Vectashield containing DAPI (Vector laboratories) and examined under a Zeiss Axioplan fluorescence microscope.

Conjugation of IF7C(RR) with SN-38. SN-38 was provided by Yakult Honsha. Conjugation of synthetic peptide with SN-38 was performed as described by Meyer-Losic, et al (32), except following modifications. Tranexamic acid (500 mg) was dissolved in 12.5 mL water and the pH adjusted by adding 1 mL 1 M Na-phosphate buffer, pH 6.5. One gram of succinimidyl-4-(N-maleimidomethyl)cyclohexane-1-carboxylate (SMCC; Pierce) was dissolved in a mixture of 22 mL acetonitrile and 5.5 mL water. Tranexamic acid solution was added to the SMCC solution and incubated at 45 °C for 2 h. Then, 20 mL of a 2:1 (vol/vol) mixture of dichlorolomethane (DCM):methanol and 60 mL DCM (60 mL) were added, and the organic phase was washed with 20 mL of 0.1 M NaCl. After removing the aqueous (upper) phase, the organic phase was washed twice with 5 mL each of water and evaporated using a rotary evaporator. The dried material was dissolved with 9 mL DCM:methanol (2:1) and 40 mL methyl tert-butyl ether, and left at −20 °C overnight. A white precipitate 4-{4-[(N-maleimydomethyl)cyclohexanecarboxamido]-methyl} cyclohexane-1-carboxylic acid linker (BCH) was collected by centrifugation. The structure of BCH was confirmed by mass spectrometry (Waters, Micromass ZQ 2000). IF7C(RR)-BCH-SN38 forming a semisold interphase was collected by decantation, suspended in water, and completely dried in a vacuum. Crude IF7C(RR)-BCH-SN38 was dissolved in 50% acetonitrile/water and purified by using a C18 reverse-phase HPLC column (10×150 mm) in HPLC (Shimadzu LC-10AD) by elution in a linear gradient from 50% to 70% acetonitrile in water containing 0.01% trifluoro acetic acid over 20 min at a flow rate of 2.5 mL/min. The purity and structure of IF7-SN38 was assessed by ESI mass spectrometry. The purity of IF7C(RR)-SN38 and RQ7C(RR)-SN38 was 98.33% and 99.39%, respectively.

Generation of HCT116-Luc Cells and HCT116-Luc Tumor Monitoring. Human colon carcinoma HCT116 cells were cultured in Dulbecco's Modified Eagle's (DME) plus high glucose medium containing 10% fetal bovine serum. The lentiviral plasmid vector CSII-Luc was constructed and provided by Nikunj Somia of the University of Minnesota. HCT116 cells were infected with CSII-Luc virus to produce luciferase positive HCT116-Luc cells. HCT116-Luc cells were trypsinized, suspended in DME medium containing 1 mg/mL Matrigel (Beckton-Dickenson), and cell suspension (50 μL, 5×10^5 cells) was injected subcutaneously into 8–10 w-old female nu/nu mice. Six days later, mice were subjected to imaging for luciferase-expressing tumors: 100 μL luciferin (30 mg/mL PBS) was injected into the peritoneal cavity of the mouse. Mice were then anesthetized under isoflurane gas (20 mL/min) supplemented with oxygen (1 mL/min) and placed under a camera equipped with a Xenogen IVIS 200 imager. Photon numbers were measured for 1–10 s.

ACKNOWLEDGMENTS. The authors thank Drs. Erkki Ruoslahti and Jan E. Schnitzer for critical reading of an early version of the manuscript and valuable suggestions. We thank Drs. Katsushige Gomi and Takashi Yaegashi of Yakult Honsha, Co. Ltd, for their valuable suggestions about use of SN-38. We thank Dr. Elise Lamar for editing the manuscript and Merrill Mathew for technical assistance. This study has been supported by National Institutes of Health (NIH) Grant P01CA071932 (M.F. and M.N.F.), Department of Defense (DoD) Breast Cancer Research IDEA Grant DAMD17-02-1-0311 (M.N.F.), and a Susan Komen Breast Cancer Research Grant BCTR0504175 (M.N.F.).

1. Hakomori S (2002) Glycosylation defining cancer malignancy: new wine in an old bottle. *Proc Natl Acad Sci USA* 99:10231–10233.
2. Nakamori S, et al. (1993) Increased expression of sialyl Lewisx antigen correlates with poor survival in patients with colorectal carcinoma: clinicopathological and immunohistochemical study. *Cancer Res* 53:3632–3637.
3. Fukuda MN, et al. (2000) A peptide mimic of E-selectin ligand inhibits sialyl Lewis X-dependent lung colonization of tumor cells. *Cancer Res* 60:450–456.
4. Fukuda MN (2006) Screening of peptide-displaying phage libraries to identify short peptides mimicking carbohydrates. *Methods Enzymol* 416:51–60.
5. Taki T, et al. (2008) A new approach for drug discovery from glycobiology and phage-displayed peptide library technology. *Biochim Biophys Acta* 1780:497–503.
6. Scott JK, Loganathan D, Easley RB, Gong X, Goldstein IJ (1992) A family of concanavalin A-binding peptides from a hexapeptide epitope library. *Proc Natl Acad Sci USA* 89:5398–5402.
7. Molenaar TJ, et al. (2002) Specific inhibition of P-selectin-mediated cell adhesion by phage display-derived peptide antagonists. *Blood* 100:3570–3577.
8. Kieber-Emmons T, et al. (1999) Vaccination with carbohydrate peptide mimotopes promotes anti-tumor responses. *Nat Biotechnol* 17:660–665.
9. O I, Otvos L, Kieber-Emmons T, Blaszczyk-Thurin M (2002) Role of SA-Le(a) and E-selectin in metastasis assessed with peptide antagonist. *Peptides* 23:999–1010.
10. Ohyama C, Tsuboi S, Fukuda M (1999) Dual roles ofsialyl Lewis X oligosaccharides in tumor metastasis and rejection by natural killer cells. *Embo J* 18:1516–1525.

11. Zhang J, et al. (2002) Sialyl Lewis X-dependent lung colonization of B16 melanoma cells through a selectin-like endothelial receptor distinct from E- or P-selectin. *Cancer Res* 62:4194–4198.
12. Hatakeyama S, et al. (2009) Identification of mRNA splicing factors as the endothelial receptor for carbohydrate-dependent lung colonization of cancer cells. *Proc Natl Acad Sci USA* 106:3095–3100.
13. Ruoslahti E, Rajotte D (2000) An address system in the vasculature of normal tissues and tumors. *Annu Rev Immunol* 18:813–827.
14. Neri D, Bicknell R (2005) Tumour vascular targeting. *Nat Rev Cancer* 5:436–446.
15. Oh P, et al. (2004) Subtractive proteomic mapping of the endothelial surface in lung and solid tumours for tissue-specific therapy. *Nature* 429:629–635.
16. Gerke V, Creutz CE, Moss SE (2005) Annexins: linking Ca^{2+} signalling to membrane dynamics. *Nat Rev Mol Cell Biol* 6:449–461.
17. Rescher U, Gerke V (2004) Annexins—unique membrane binding proteins with diverse functions. *J Cell Sci* 117:2631–2639.
18. Perretti M, et al. (1996) Mobilizing lipocortin 1 in adherent human leukocytes down-regulates their transmigration. *Nat Med* 2:1259–1262.
19. Perretti M, Flower RJ (2004) Annexin 1 and the biology of the neutrophil. *J Leukocyte Biol* 76:25–29.
20. Hannon R, et al. (2003) Aberrant inflammation and resistance to glucocorticoids in annexin 1-/- mouse. *Faseb J* 17:253–255.
21. Lehr HA, Leunig M, Menger MD, Nolte D, Messmer K (1993) Dorsal skinfold chamber technique for intravital microscopy in nude mice. *Am J Pathol* 143:1055–1062.
22. Vasilevskaya IA, Rakitina TV, O'Dwyer PJ (2003) Geldanamycin and its 17-allylamino-17-demethoxy analogue antagonize the action of Cisplatin in human colon adenocarcinoma cells: differential caspase activation as a basis for interaction. *Cancer Res* 63:3241–3246.
23. Mandler R, et al. (2000) Immunoconjugates of geldanamycin and anti-HER2 monoclonal antibodies: antiproliferative activity on human breast carcinoma cell lines. *J Natl Cancer Inst* 92:1573–1581.
24. Eiseman JL, et al. (2005) Pharmacokinetics and pharmacodynamics of 17-demethoxy 17-[[(2-dimethylamino)ethyl]amino]geldanamycin (17DMAG, NSC 707545) in C.B-17 SCID mice bearing MDA-MB-231 human breast cancer xenografts. *Cancer Chemother Pharmacol* 55:21–32.
25. Solit DB, et al. (2002) 17-Allylamino-17-demethoxygeldanamycin induces the degradation of androgen receptor and HER-2/neu and inhibits the growth of prostate cancer xenografts. *Clin Cancer Res* 8:986–993.
26. Mitsiades CS, et al. (2006) Antimyeloma activity of heat shock protein-90 inhibition. *Blood* 107:1092–1100.
27. Solit DB, Basso AD, Olshen AB, Scher HI, Rosen N (2003) Inhibition of heat shock protein 90 function down-regulates Akt kinase and sensitizes tumors to Taxol. *Cancer Res* 63:2139–2144.
28. Clarke PA, et al. (2000) Gene expression profiling of human colon cancer cells following inhibition of signal transduction by 17-allylamino-17-demethoxygeldanamycin, an inhibitor of the hsp90 molecular chaperone. *Oncogene* 19:4125–4133.
29. Panaretou B, et al. (2002) Activation of the ATPase activity of hsp90 by the stress-regulated cochaperone aha1. *Mol Cell* 10:1307–1318.
30. Kawato Y, Aonuma M, Hirota Y, Kuga H, Sato K (1991) Intracellular roles of SN-38, a metabolite of the camptothecin derivative CPT-11, in the antitumor effect of CPT-11. *Cancer Res* 51:4187–4191.
31. van Ark-Otte J, et al. (1998) Determinants of CPT-11 and SN-38 activities in human lung cancer cells. *Br J Cancer* 77:2171–2176.
32. Meyer-Losic F, et al. (2008) DTS-108, A novel peptidic prodrug of SN38: in vivo efficacy and toxicokinetic studies. *Clin Cancer Res* 14:2145–2153.
33. Motwani M, et al. (2001) Augmentation of apoptosis and tumor regression by flavopiridol in the presence of CPT-11 in Hct116 colon cancer monolayers and xenografts. *Clin Cancer Res* 7:4209–4219.
34. Izumoto S, et al. (2008) Phase II clinical trial of Wilms tumor 1 peptide vaccination for patients with recurrent glioblastoma multiforme. *J Neurosurg* 108:963–971.
35. Schnitzer JE, Liu J, Oh P (1995) Endothelial caveolae have the molecular transport machinery for vesicle budding, docking, and fusion including VAMP, NSF, SNAP, annexins, and GTPases. *J Biol Chem* 270:14399–14404.
36. Oh P, et al. (2007) Live dynamic imaging of caveolae pumping targeted antibody rapidly and specifically across endothelium in the lung. *Nat Biotechnol* 25:327–337.
37. Otvos L, Jr (2008) Peptide-based drug design: here and now. *Methods in Molecular Biology* 494:1–8.
38. Landon LA, Zou J, Deutscher SL (2004) Is phage display technology on target for developing peptide-based cancer drugs? *Current Drug Discovery Technologies* 1:113–132.
39. Gerke V, Moss SE (2002) Annexins: from structure to function. *Physiol Rev* 82:331–371.